Numerical Characterization of Bone Defects After Dental Implantation[1]

Bin-Xun Hsieh
Graduate Institute of Biomedical Engineering,
National Central University,
No. 300, Jhongda Rd.,
Jhongli City, Taoyuan 32001, Taiwan

Chin-Sung Chen
Department of Dentistry,
Sijhih Cathy General Hospital,
Taiwan

Min-Chun Pan
Graduate Institute of Biomedical Engineering;
Department of Mechanical Engineering,
National Central University,
No. 300, Jhongda Rd.,
Jhongli City, Taoyuan 32001, Taiwan
e-mail: pan_minc@cc.ncu.edu.tw

1 Background

Two stages of stability are in the healing phase of dental implantation, i.e., the primary and the secondary stability. The former refers to the stability immediately after implantation. The most critical occasion for achieving successful implantation occurs during the lowest initial stabilization that causes sufficient bone reconstruction to support long-term maintenance of the implant. Usually this occurs in the third or the fourth week after surgery [1]. If the primary stability is not high enough, the extra implant mobility may cause bone defects and result in implantation failed eventually. In the former studies, varied techniques, especially resonance frequency analysis (RFA), were developed for quantifying dental implant stability including experimental and numerical ways [2–4]. In terms of numerical characterization, Wang et al. [2] determined the identifiable stiffness range of interfacial tissue of dental implants by using RFA. Two implant-tissue-bone models were built and analyzed by finite element method (FEM). They found when Young's modulus of interfacial tissue is less than 15 MPA, the RF is significantly affected by the interfacial tissue rather than boundary constrains or geometry variations. Li et al. [3] assessed the changes of the RF during the bone remodeling through three-dimensional time-dependent finite-element simulation. A quantitative comparison was made with the measured RFs from the clinical follow-ups. The comparison demonstrated a satisfactory agreement between the simulation of developed bone remodeling and clinical data. Zhuang et al. [4] conducted finite element (FE) modal analysis to validate the measured RF through a noncontact vibro-acoustic detection technique. A comparison of bone block model experiments with numerical simulation showed that the RFs in the defect side are significantly smaller than those in the complete one, as well as the value decreasing with the increase of defect amount.

In the past studies, the findings showed overall peri-implant assessment mainly, and were lack of comprehensive information about the effects of bone defect severity on stability during the healing phase. To the end this technical brief explores the effect of both the severities of closed bone defects and interfacial tissue on the corresponding resonance frequencies (RFs) of dental-implanted structure.

2 Methods

Bone defects adjacent to dental implant are categorized into two groups, closed defects and open defects. For the closed defects, vertical and horizontal bone defects are named as Class I and Class II defects, respectively. In the study, Class I defects with 1–5 mm depth and 1 mm width, as shown in Fig. 1, were analyzed numerically, and Class II defects with 2 and 3 mm depth and 1–5 mm width were investigated (Fig. 2). The surrounding interfacial tissue for the primary stability was considered with the Young's modulus of 10 MPa in the simulation of bone defects.

The full mandible model with a dental implant and interfacial tissue, as shown in Fig. 3, was built by using an FEM commercial package, ANSYS Workbench. The analyzed mandible model is composed of cortical bone and cancellous bone, in which the former has an average thickness of 2 mm. A cylindrical implant socket (Φ5.7 mm $\times$ 12 mm) was modeled as a drilled hole to accommodate the dental implant (Φ3.7 mm $\times$ 9 mm), where a layer of 1 mm thickness surrounding the implant was created as the interfacial tissue for the simulation of the osseointegration phase. Furthermore, in the model an aluminum peg is screwed to the implant. In the modeling of RFA, here the whole implant/interfacial-tissue/bone (IITB) is regarded as a system. The material properties of different parts are simplified and assumed isotropic and homogeneous, as summarized in Table 1 [5,6]. The interfaces between each two subparts were assumed bonded. Three combinations of material properties are designated as shown in Table 2. They are synthesized using the material properties of Table 1 to imitate the variety of individual gum structure. During the primary stability stage, the Young's modulus of the tissue changes from 1 MPa to 25 MPa. In the simulation of primary and secondary stability the Young's modulus of the tissue changes from 5 MPa to 100 MPa in eleven levels. The FE model contains

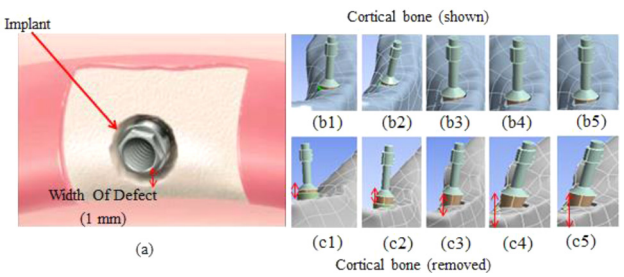

Fig. 1 Class I closed defects with surrounding bone walls. (*a*) Birdview of implant with 1 mm width closed defect, and with a depth of (b1) 1, (b2) 2, (b3) 3, (b4) 4, and (b5) 5 mm. (c1)–(c5) with cortical bone removed correspond to (b1)–(b5).

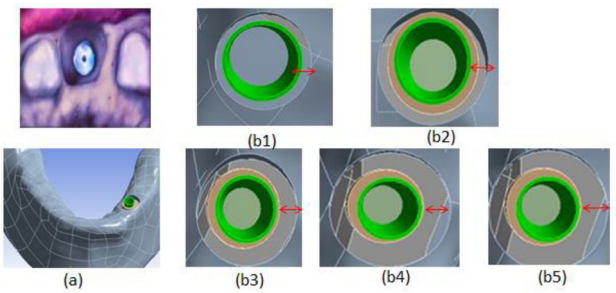

Fig. 2 Class II closed defects with surrounding bone walls. (*a*) Birdview of implant with 2 or 3 mm depth closed defect, and with a width of (b1) 1, (b2) 2, (b3) 3, (b4) 4, and (b5) 5 mm surrounding the implant.

[1]Accepted and presented at the Design of Medical Devices Conference (DMD2014), Minneapolis, MN, April 7–10, 2014.
DOI: 10.1115/1.4027049
Manuscript received February 21, 2014; final manuscript received March 3, 2014; published online April 28, 2014. Editor: Arthur G. Erdman.

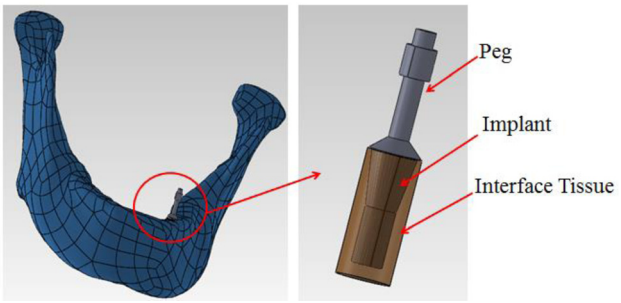

Fig. 3 Finite element model of designated IITB system including test peg, implant, interfacial tissue, and mandible

Table 1 Material property range of designated IITB system

	Young's modulus (MPa)	Density (kg/m^3)	Poisson's ratio
Ti (implant)	113,800	4480	0.34
Al (peg)	70,500	2780	0.35
Cortical bone	11,580–34,740	930.1–2790.2	0.321–0.421
Cancellous bone	411.5–1234.5	355.98–1067.92	0.2636–0.3636
Interfacial tissue	5–100	1500	0.22

Table 2 Designated material properties of the three bone-structure combinations

Combin_		Young's modulus (MPa)	Density (kg/m^3)	Poisson's ratio
1	Cortical 1	11,580	930.1	0.321
	Cancellous 1	411.5	355.98	0.2636
2	Cortical 2	23,160	1860.1	0.371
	Cancellous 1	823	711.95	0.3136
3	Cortical 1	34,740	2790.2	0.421
	Cancellous 1	1234.5	1067.92	0.3636

15,270 tetrahedral solid elements and 29,478 nodes with the element size of 5 mm based upon convergence analysis. Free-free boundary conditions are set [6]. The harmonic force with 1 Pa acoustic pressure was applied on the peg, and the vibration response on the opposite side was computed. Figure 1: Class I closed defects with surrounding bone walls. (a) Birdview of implant with 1 mm width closed defect, and with a depth of (b1) 1, (b2) 2, (b3) 3, (b4) 4, and (b5) 5 mm. (c1)–(c5) with cortical bone removed correspond to (b1)–(b5).

3 Results

In the three bone-structure combinations, Combin_3 has the stiffest material properties; contrarily, Combin_1 is the most flexible. From the results of modal analysis, Fig. 4 shows the RFs decrease along the severity of closed-defect depth. It is noted that the RFs of Combina_1 and Combin_2 almost coincide when the depth of closed defect is in one mm. When the depth of closed defects is larger than one mm, the differences among RFs of the three combination models become significant. It is consistent that Combin_3 bone structure always keeps the highest RFs. Further, the percentages of frequency decrement are below 10% in one mm defect depth, and become larger when the defects become more severe. The largest frequency decrease goes up to 51% at Combin_1 bone structure with 5 mm defect depth. As to the RF

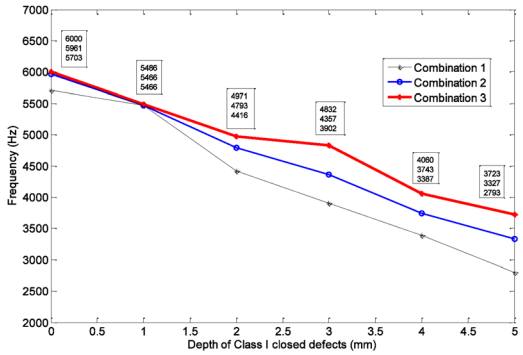

Fig. 4 RF trend of three combinations models with Class I closed defects, where all defect width is1 mm

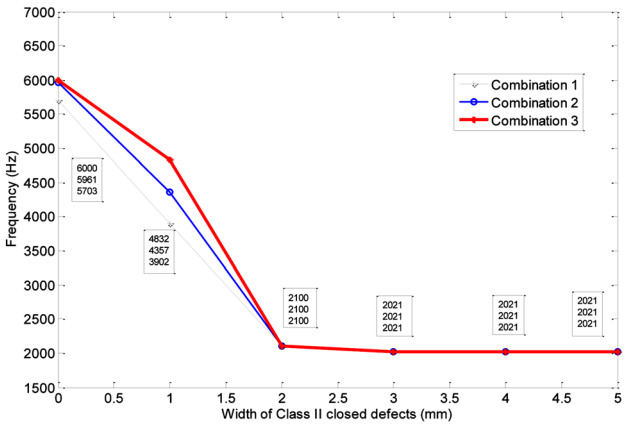

Fig. 5 RF trend of three combinations models with Class II closed defects, where all defect depth is 3 mm

variation of Class II closed defects, Fig. 5 shows the structural resonance ranges from 6000 Hz to 2021 Hz along with defect severity. When the defect width is over 2 mm, the RFs stay steady for whatever combination models.

From the analysis of bone-defect severity it is concluded that the defect width damages stability dramatically, and the bone defect harms the stability consistently along its depth. However, it is noted that the sufficient stability of an implant still varies individually; from the analysis, it ranges between 5500 and 6000 Hz.

References

[1] Glauser, R., Sennerby, L., Meredith, N., Rèe, A., Lundqen, A., Gottlow, J., and Hämmerle, C., 2004, "Resonance Frequency Analysis of Implants Subjected to Immediate or Early Functional Occlusal Loading," Clin. Oral Implants Res., **15**(4), pp. 428–434.

[2] Wang, S., Liu, G. R., Hoang, K. C., and Guo, Y., 2010, "Identifiable Range of Osseointegration of Dental Implants Through Resonance Frequency Analysis," Med. Eng. Phys., **32**(10), pp. 1094–1096.

[3] Li, W., Lin, D., Chaiy, R., Zhou, S., Michael, S., and Li, Q., 2011, "Finite Element Based Bone Remodeling and Resonance Frequency Analysis for Osseointegration," Finite Elem. Anal. Des., **47**(8), pp. 898–905.

[4] Zhuang, H. B., Tu, W. S., Pan, M. C., Wu, J. W., Chen, C. S., Lee, S. Y., and Yang, Y. C., 2013, "Noncontact Vibro-Acoustic Detection Technique for Dental Osseointegration Examination," J. Med. Biol. Eng., **33**(1), pp. 35–44.

[5] Wang, S., Liu, G. R., Hoang, K. C., and Guo, Y., 2010, "Identifiable Range of Osseointegration of Dental Implants Through Resonance Frequency Analysis," Med. Eng. Phys., **32**(10), pp. 1094–1096.

[6] Lacroix, D., Prendergast, P. J., Li, G., and Marsh, D., 2002, "Biomechanical Model to Simulate Tissue Differentiation and Bone Regeneration: Application to Fracture Healing," Med. Biol. Eng. Comput., **40**(1), pp. 14–21.